

# Stability of Te-O-H based materials from density functional theory

Laurent Simons

*TQC, Universiteit Antwerpen, Universiteitsplein 1, B-2610 Antwerpen, Belgium*

Kushal Samanta and Robrecht Jennen

*Department of Materials, Textiles And Chemical Engineering, Ghent University, Belgium*

José Devienne

*Department of Geophysics, School of Earth and Space Sciences, Peking University, China*

## Abstract

In this report the stability of a few Te-O-H-based crystals and molecules is discussed. The formation energy of such structures is obtained based on density functional theory (DFT) calculations, which further allowed to estimate the stability of each structure, that can be graphically represented in the so-called phase diagram. This reports describe the complete procedure of using DFT to predict properties (in our case, the final total energy) of both crystals and molecules. Based on DFT results,  $\text{TeO}_2$  crystal has a formation energy of  $-0.97951$  eV/atom, above the convex hull in the phase diagram, indicating that the material is unstable at 0 K and should, therefore, decompose into a stable component. Ozone-like  $\text{TeO}_2$  molecule formation energy based on DFT prediction is  $-0.22946$  eV/atoms, whereas for the water-like  $\text{TeH}_2$  molecule the formation energy is  $0.90923$  eV/atom. The formation of both structures is energetically favourable compared to their elemental phases, however they are still above the convex hull in the phase diagram, indicating that they should decompose into new stable structures.

## I. INTRODUCTION

Since its discovery in 1898 by Pierre and Marie Curie using a radiochemical separation method, Polonium (Po), named after their native Poland and for which they both received the Nobel Prize, has sparked interest among many researchers [1–6]. It is a very rare element to occur in nature due to the short half lives of all its isotopes [7], making its isolation from natural sources a laborious process. In laboratory this element can be produced by irradiating bismuth (Bi) with high-energy neutrons or protons [8], and its industrial use covers a range of applications, from the measurement of industrial coating via attenuation of alpha radiation using Po-based source of alpha particles [8], to the use as a source of heat for spacial instruments [8, 9].

Due to its highly toxic and radioactive properties, experiments involving Po are quite difficult to be performed [1–6]. From a computational standpoint, calculation involving Po-based materials are rather difficult as well, since heavy atoms present high relativistic effect [9], making non-relativistic methods unsuitable for reliably predicting Po-based materials behaviours. However, Tellurium (Te), a (lighter) chemically analogous element to Po with similar characteristics, and mainly known for its industrial use as an alloying agent in metallurgy, enables researchers to study Te-based materials as a proxy to gain insights on the behaviour of Po-based materials without the toxic and radioactive burden [1–6]. Therefore, the investigation of Te-O-H molecules, both experimentally and computationally, can serve as an excellent candidate to obtain supporting data of Po-based molecules, as men-

tioned in the task description [1–6].

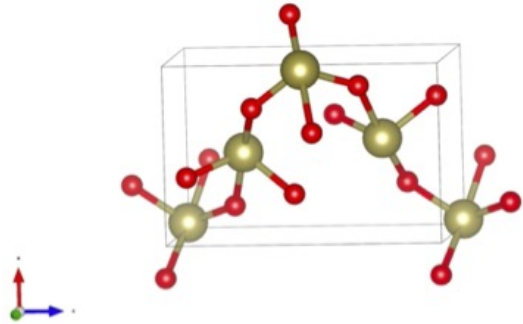


Figure 1: The  $\text{TeO}_2$  557 crystal structure is displayed using VESTA. The yellow spheres represent Te atoms and the red spheres represent O atoms.

Our contribution is to investigate, through density functional theory (DFT), the stability of Te-O-H materials. The  $\text{TeO}_2$  crystalline structure, a water-like  $\text{TeH}_2$  molecule and an ozone-like  $\text{TeO}_2$  molecule were investigated, using *ab initio* models, as a mean of predicting their formation energy. Defined the formation energies, as well as the energy required to form each elemental phase (Te,  $\text{O}_2$  and  $\text{H}_2$  separately), the stability of each structure can be assessed and graphically represented in a phase diagram.

The rest of paper is structured as follow. Section II describes the computational methods. Section III presents the results. In section IV the main conclusions and outcomes are discussed.

## II. COMPUTATIONAL METHODS

Density functional theory calculations were conducted using Quantum Espresso (QE) [2, 3]. In the QE suite of codes, core-valence electrons are accounted for based on the pseudo-potential and plane-wave basis set approach. All calculations were implemented using the generalized gradient approximation (GGA) and the exchange-correlation functional adopted was the Pedrew-Burke-Erzenhof functional (PBE).

The original crystal structure of  $\text{TeO}_2$  was retrieved from *materialsproject* website [10]. All concerned relaxations were performed utilizing the BFGS algorithm [6]. The structures (initial and relaxed) were analysed graphically using the softwares XCrySDen [11] and VESTA [12]. The pseudo-potentials files for all elements are provided with recommended values for the cut-off energy values for both basis-set of wave functions and for density. These values supplement the first step of the convergence testing protocol by taking the common maxima from both pseudo-potentials for both elements. For the molecules, the crystallographic files were created based on the  $\text{H}_2\text{O}$  and  $\text{O}_3$  molecules.

## III. RESULTS

### A. Convergence testing

To obtain meaningful information from DFT calculation, it is necessary to previously define the set of optimized parameters (namely, k-mesh size and basis-set sizes) that gives converged results for the hydrostatic pressure (a property obtained with DFT and that is strongly dependent of these parameters). Naturally, the higher the precision, the longer the computational time required to run the simulations. Therefore, this trade off between precision and computational cost was also taken into account for choosing the proper set of parameters. The convergence of the hydrostatic pressure is interpreted as that when fluctuations are less than 1 kBar.

Figures 2a and 2b shows how the hydrostatic pressure (in kBar) changes as the k-mesh size and the wave functions basis-set size (ecutwfc) varies, respectively. Based on figure 2a, from a k-mesh size of  $3 \times 3 \times 3$  onward the convergence of the hydrostatic pressure is achieved. For safety, a  $5 \times 5 \times 5$  k-mesh size was adopted for the further calculations.

Defined the proper k-mesh size, the convergence regarding the wave function basis-set was conducted. For this test, the proportion between the basis-set sizes for the wave function (ecutwfc) and for the density (ecutrho) was kept constant and equal to 6.6 (i.e.,  $\text{ecutrho} = 6.6 \times \text{ecutwfc}$ ). In Figure 2 it is notable that the hydrostatic pressure no longer varies beyond  $\pm 1$  kbar for values of  $\text{ecutwfc} \geq 50$  Ry. Based on that, a cut-off value of 60 Ry was considered the optimum for ecutwfc.

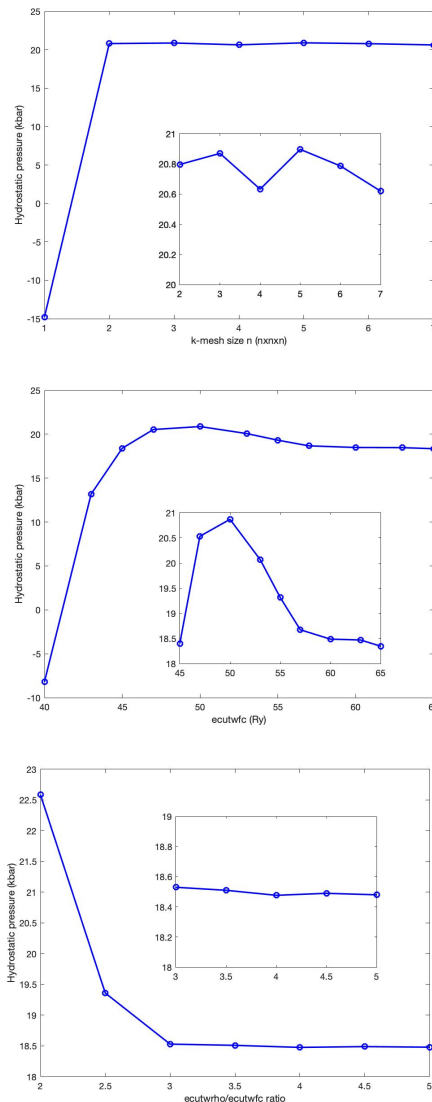


Figure 2: The hydrostatic pressure as a function of the k-mesh size, ecutwfc and the ratio between ecutrho and ecutwfc. The inset shows the fluctuations for large parameter values. Clear convergence can be seen at k-mesh size, ecutwfc and ecutrho of  $5 \times 5 \times 5$ , 60, 240 respectively.

The final step of the convergence test consists in assessing the optimum proportion factor between ecutrho and ecutwfc. For this test the optimized values for the k-mesh size ( $5 \times 5 \times 5$ ) and the wave functions basis-set size (60 Ry) were used. The density basis-set energy cut-off was varied such that the proportion factor  $f$  ( $= \text{ecutrho}/\text{ecutwfc}$ ) varied from 2 to 5. As illustrated in figure 2c, the convergence of the hydrostatic pressure is achieved for  $f \geq 3$ . For safety, a proportion factor equal to 4 (i.e.,  $\text{ecutrho} = 240$  Ry) was consider as the proper value for ecutrho.

## B. Geometrical Optimization of TeO<sub>2</sub> crystal

Considering the optimized set of parameters obtained in the convergence testing, the next step consists in performing the full geometry optimization on the TeO<sub>2</sub> crystal. This includes finding new optimal cell parameters, unit cell volume and atomic positions in the absence of external pressure. In QE this is accomplished by using the ‘vc-relax’ method, where ‘vc’ stands for ‘variable-cell’. This function automatically varies all the aforementioned parameters while trying to minimize the total energy for a given pressure.

From the ‘vc-relax’ calculation, the new optimized lattice parameters for the TeO<sub>2</sub> crystal were found to be  $a = b = 4.97167 \text{ \AA}$  and  $c = 7.58012 \text{ \AA}$ . The new unit cell volume is then  $187.36214 \text{ \AA}^3$ . Apart from the calculation of the optimized geometry for the TeO<sub>2</sub>, in order to get the formation energy of this crystal, the knowledge of the total energy of the elemental phases of Te and O<sub>2</sub> is necessary. In table 1 the optimized volume and the corresponding total energy of TeO<sub>2</sub>, Te, O<sub>2</sub> and H<sub>2</sub> (useful in the next section) are presented.

Table I: The optimized volume and the corresponding total energy of TeO<sub>2</sub>, Te and O<sub>2</sub> obtained with QE ‘vc-relax’ calculation.

Structure	Volume ( $\text{\AA}^3$ )	Total energy (Ry)
TeO <sub>2</sub>	187.36214	-1783.4313
Te	105.09541	-1087.8239
O <sub>2</sub>	135.74972	-332.17183
H <sub>2</sub>	31.263	-2.3333

The formation energy of TeO<sub>2</sub> is determined as follow:

$$\begin{aligned} E_{form}/atom &= \frac{E_{TeO_2} - (n_{Te} \times E_{Te} + n_{O_2} \times E_{O_2})}{(n_{Te} + n_{O_2})_{TeO_2}} \\ &= -0.97951 \text{ eV/atom} \end{aligned} \quad (1)$$

with  $E_{TeO_2}$ ,  $E_{Te}$  and  $E_{O_2}$  the total energy for TeO<sub>2</sub>, Te and O<sub>2</sub>, respectively, as presented in table 1;  $n_{Te}$  (=3) the number of atoms in the unit cell of Te crystallographic file,  $n_{O_2}$  (=8) the number of atoms in O<sub>2</sub> unit cell, and  $(n_{Te} + n_{O_2})_{TeO_2}$  the number of atoms in TeO<sub>2</sub> unit cell (= 12, 4 Te and 8 O).

To determine the stability of a crystal, the formation energy of all possible lowest energy structures are required. Plotting the formation energy for different atomic fraction of Te and O<sub>2</sub> allows to determine a phase diagram. The convex hull is constructed by connecting the lowest points on the phase diagram, respecting no concave angles between lines are allowed. This construction makes it possible to determine the stability of a structure. If a point lies above the convex hull, its structure is unstable, i.e. another structure is energetically favored. The phase diagram and the convex hull for TeO<sub>2</sub> is shown in figure 3

The formation energy obtained from DFT calculations (-0.97951 eV/atom) deviate in 34.4 % to the one found on *materialsproject* website (-1.494 eV/atom). The use of different pseudo potential files, for instance, may represents a possible cause for this deviation, but qualitatively both results agree to predict an unstable structure. This formation energy value for the TeO<sub>2</sub> crystal lies just above the convex hull of the phase diagram (Figure 3), indicating that this structure is energetically unfavourable.

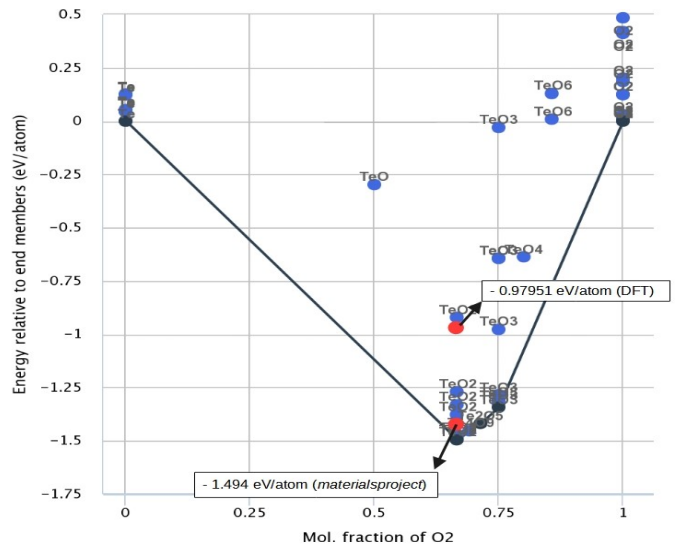


Figure 3: Te-O phase diagram from *materialsproject*.

## C. Stability of Te-O-H based molecules

DFT codes as QE (i.e., typically meant for solid state calculations) can be used to investigate molecules by making use of the supercell concept. A supercell is created by increasing the lattice parameter in such a way that the molecules do not interact with each other (i.e., a free molecule). The energy retrieved as a function of the supercell length is shown in Figure 4 for both TeH<sub>2</sub> and TeO<sub>2</sub> molecules. As presented in figure 4, above 12  $\text{\AA}$  the energy no longer changes. Again for safety, a length of 15  $\text{\AA}$  was adopted. Table 2 presents the total energy, the angle and bond length for the molecules. From this values it was possible to obtain the formation energy TeO<sub>2</sub> (-0.22946 eV/ atoms) and TeH<sub>2</sub> (0.90923 eV/ atom) molecules.

Table II: Bond angle, length and total energy for TeH<sub>2</sub> and TeO<sub>2</sub> molecules.

Structure	Bond angle ( $^\circ$ )	Bond length ( $\text{\AA}$ )	Total energy (Ry)
TeH <sub>2</sub>	89.686	1.677	-364.8785
TeO <sub>2</sub>	111.117	1.8299	-445.69847

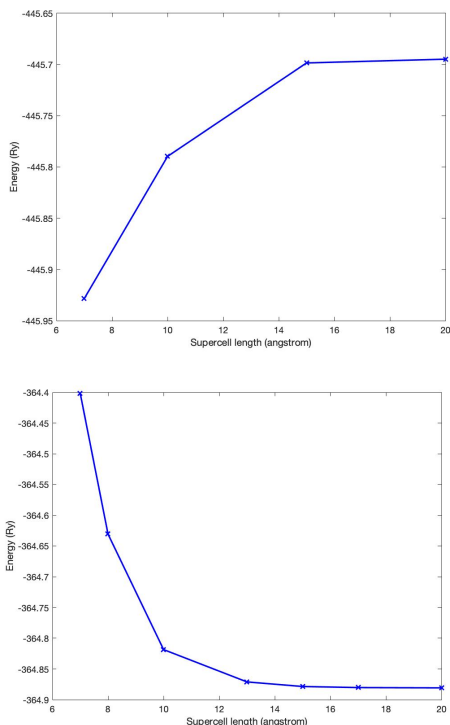


Figure 4: The energy of the two molecules (a) TeO<sub>2</sub> and (b) TeH<sub>2</sub> as a function of the supercell size length. The optimal supercell size length is approximately 15 Å.

## IV. CONCLUSIONS

Based on *ab initio* results, it was possible to assess the stability of a TeO<sub>2</sub> crystal structure as well as of two molecules (TeH<sub>2</sub> and TeO<sub>2</sub>) from the Te-O-H family of molecules. Even though the DFT predictions presented here deviates from the ones predicted in *materialsproject*, the qualitative information is still in agreement: the mp-557 TeO<sub>2</sub> is unstable, although it represents an energy gain from its elemental phases. In addition to the crystal structures, the molecular structures were also investigated with the DFT. Based on the DFT results, the TeO<sub>2</sub> crystal structure is favored energetically compared to the ozone-like TeO<sub>2</sub> molecule one. For TeH<sub>2</sub>, the positive formation energy indicates that the structure is not likely do occur spontaneously from the elemental phases. The results obtained in this report from a few Te-based structures based on *ab initio* modeling can serve as candidate to obtain supporting data for further studies with Po-based structures, now considering a full-relativistic approach (as discuss in the project description).

## ACKNOWLEDGMENTS

The authors would like to thank Prof. dr. S. Cottelier for the opportunity to follow this interactive course and for the excellent mentorship with the weekly feedback seminars and in the feedback forms.

- 
- [1] E. Ansoforlo, Poisonous polonium, *Nature Chemistry* **6**, 454 (2014).
  - [2] S. e. a. Ohno, Equilibrium evaporation behavior of polonium and its homologue tellurium in liquid lead-bismuth eutectic, *Journal of Nuclear Science and Technology* **43**, 1359 (2006).
  - [3] J. e. a. Neuhausen, Investigation of evaporation characteristics of polonium and its lighter homologues selenium and tellurium from liquid pb-bi-eutecticum, *Radiochimica Acta* **92** (2004).
  - [4] A. Downs, Selenium, tellurium and polonium, *Nature* **212**, 1190 (1966).
  - [5] S. Patai, Rappoport, and H. Gysling, *The chemistry of organic selenium and tellurium compounds volume 1 edited ligand properties of organic selenium and tellurium compounds* (2019).
  - [6] J. Ibers, Tellurium in a twist, *Nature Chemistry* **1**, 508 (2009).
  - [7] R. Collé and P. -. Fitzgerald, *R*, **41**, 105103 (2014).
  - [8] W. e. a. Schulz, Pyrochemical extraction of polonium from irradiated bismuth metal, *Industrial & Engineering Chemistry Process Design and Development* **8**, 508 (1969), <https://doi.org/10.1021/i260032a013>.
  - [9] V. e. a. Srinivasadesikan, *Applications of Density Functional Theory on Heavy Metal Sensor and Hydrogen Evolution Reaction (HER)*, **1**, p. 011002.
  - [10] J. e. a. Anubhav, The Materials Project: A materials genome approach to accelerating materials innovation, *APL Materials* **1**, 011002 (2013).
  - [11] A. Kokalj, Computer graphics and graphical user interfaces as tools in simulations of matter at the atomic scale, *Comp. Mater. Sci.* **28**, 155 (2003).
  - [12] K. Momma and F. Izumi, *VESTA3* for three-dimensional visualization of crystal, volumetric and morphology data, *Journal of Applied Crystallography* **44**, 1272 (2011).
  - [13] P. G. et al., Advanced capabilities for materials modelling with quantum espresso, *Journal of Physics: Condensed Matter* **29**, 465901 (2017).
  - [14] P. e. a. Giannozzi, Quantum espresso: a modular and open-source software project for quantum simulations of materials, *Journal of Physics: Condensed Matter* **21**, 395502 (19pp) (2009).
  - [15] P. e. a. Giannozzi, Quantum espresso toward the exascale, *The Journal of Chemical Physics* **152**, 154105 (2020).